Kinetic evidence for protein clustering at a surface

J.J. Ramsden*
Department of Biophysical Chemistry, Biozentrum, 4056 Basel, Switzerland

G.I. Bachmanova and A.I. Archakov
Institute of Biological and Medical Chemistry, Russian Academy of Medical Sciences, 10, Pogodinskaya Street, 119832 Moscow, Russia
(Received 27 July 1994)

The molecules designated 1A2 and 2B4 belong to the cytochrome P450 protein superfamily. They can interact specifically with lipid bilayers via the penetration of part of their amino acid chains into the bilayer. The kinetics of their irreversible adsorption from solution to phospholipid bilayers, accurately measured in the low to intermediate coverage range using an integrated optics reflectance technique, differ significantly: at intermediate bulk solution concentrations, 2B4 shows typical random sequential adsorption (RSA) kinetics, whereas 1A2 shows Langmuir kinetics. At higher bulk concentration the behavior of 1A2 switches to RSA kinetics, and at very low concentrations 2B4 switches to Langmuir kinetics. The Langmuir kinetics provides strong evidence for clustering of the molecules at the bilayer surface, and the observed concentration dependence of the kinetics is consistent with the clusters arising through lateral diffusion of the proteins on the surface.

PACS number(s): 87.22.−q, 68.10.Jy, 82.65.−i, 81.15.Lm

I. INTRODUCTION

The study of the adsorption of particles at surfaces, a phenomenon ubiquitous in nature, has received strong impetus with the realization that the random sequential adsorption (RSA) model [1,2] provides a good basis for describing the process. This model is simple enough to be amenable to calculations (complete analytical solutions are available for the one-dimensional case [3]), and a particularly favorable aspect of its application to problems is the fortuitious mutual cancellation of corrections taking diffusion and hydrodynamic interactions into account [4]. Good approximate expressions are available for the kinetics of adsorption in the low to intermediate coverage range (up to $\theta \approx 0.3$) [5,6] and for the asymptotic range ($\theta > 0.4$) [7,8]. They apply to rigid, incompressible hard discs adsorbing irreversibly at a planar surface. Expressions have also been derived for RSA extended by permitting desorption from the surface and diffusion on the surface [9].

Such has been the rate of progress in the theory that experiment is lagging behind, mainly due to a dearth of techniques capable of providing data accurate enough to compare with predictions, and the perennial difficulty of preparing well characterized systems. With the advent of some new techniques, this situation is now changing [10,11]; regarding the choice of particles, proteins have long been regarded with favor because of their uniformity and characterization down to the atomic level, both chemically and structurally. Proteins are far from being isotropic spheres, however, and may interact specifically with each other and certain types of surface. The P450 proteins are believed to be oblate ellipsoids of revolution, possessing in addition a small tail of nonpolar amino acids which protrudes from the main body and interacts specifically with phospholipid bilayers (Fig. 1).

In this paper we report experimental results for the adsorption of two forms of cytochrome P450, 1A2, and 2B4. These proteins are completely characterized with respect to their amino acid sequence [12], and are available in highly purified form. As an adsorbing surface, we use a lipid bilayer. This is the natural surface with which these proteins interact in living cells. By preparing bilayers on a planar support by the sequential assembly of ordered monolayers using a combination of the Langmuir-Blodgett and Langmuir-Schaefer techniques, reproducible, well characterized, and uniform surfaces can be procured. A further advantage of this system is that some independent information on the topology of

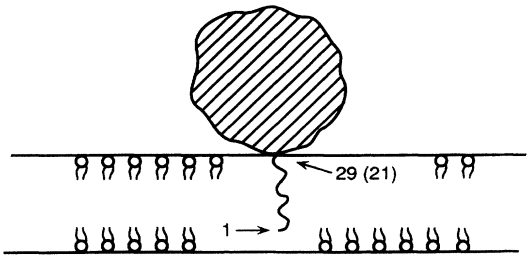

FIG. 1. Sketch of the topology of the interaction of P450 with bilayer lipid membranes. The digits mark the beginning (N-terminal, 1) and end (29 or 21 for 1A2 or 2B4, respectively, numbering the amino acids sequentially) of the nonpolar amino acid tail (see Fig. 2).

*Corresponding author.

Cytochrome P450 1A2 (N-terminal tail):

1 29

M A M S P A A P L S V T E L L L V S A V F C L V F W A V R

Cytochrome P450 2B4 (N-terminal tail):

1 21

M E F S L L L L L A F L A G L L L L L F R

FIG. 2. Membrane-penetrating tail sequences of 1A2 and 2B4. Note that all the amino acids except glutamic acid (E) are nonpolar (hydrophobic), and that E is negatively charged under the salt and pH conditions of the experiments. The rest of each molecule comprises 486 and 470 amino acids for 1A2 and 2B4, respectively [15].

the protein-bilayer interaction has recently been obtained [13,14]: the protein is anchored to the surface by a short sequence of mainly nonpolar (hydrophobic) amino acids at one end on the chain, which is deeply embedded in the bilayer and may even penetrate it (Fig. 1). The two proteins investigated differ in the length and sequence of this tail (Fig. 2). In both, only one polar amino acid, glutamic acid (E) is present, and is expected to be negatively charged under the conditions of the experiment. We have found that the two proteins show striking differences in their adsorption behavior.

II. EXPERIMENT

In order to be able to calculate accurately the number of adsorbed molecules, a planar optical waveguide was used as the adsorbing surface. The presence of a thin adlayer $\mathcal{A}$ at the waveguide-solution interface modifies the Fresnel reflexion coefficients for the interface [17] and, hence, the mode spectrum of the waveguide [10,11,18,19]. By repeatedly measuring the mode eigenvalues N, the evolution of the adlayer (consisting of adsorbed protein molecules) can be followed. An external light beam (wavelength λ) incident with an angle α onto a diffraction grating (period Λ) incorporated into the waveguide is coupled into the waveguide provided the following condition is satisfied [18,20]:

$$N = n \sin\alpha + \ell\lambda/\Lambda \,, \tag{1}$$

where n is the refractive index of air and ℓ the diffraction order. Hence the mode spectrum can be recorded with photodiodes situated at the ends of the waveguide to measure the intensity of the incoupled light as α is varied.

$Si(Ti)O_2$ waveguides (type 2400) incorporating a diffraction grating (Λ = 416.15 nm) were obtained from Artificial Sensing Instruments, Zurich, Switzerland and coated with a bilayer of dioleoylphosphatidylcholine (DOPC) using standard Langmuir-Blodgett and Langmuir-Schaefer techniques as described previously [16]. A small flow-through cuvette was clamped over the grating region such that it formed one wall of the cuvette, through which solutions could flow. The flow rate $\mathcal{F}$ (in the range 1.6–2.1 mm^3/s) was measured for each run by weighing the amount of liquid that flowed through the cuvette during a given time interval. N_{TE} and N_{TM} (corresponding to the zeroth order transverse electric and transverse magnetic modes) were determined using an IOS-1 automatic scanning goniometer (Artificial Sensing Instruments, Zurich, Switzerland) capable of an angular resolution of 1.25 μrad.

At the beginning of an experiment, N was measured with pure buffer flowing through the cuvette. Following the establishment of a stable baseline, the flowing buffer solution was replaced by flowing protein solution until the rate of deposition had markedly slowed down (log-log plots showed that a plateau was being approached). Finally the protein solution was replaced by flowing buffer solution; the fraction of adsorbed material removed never exceeded 9% . We assume this desorbed material to consist of proteins that were not properly attached to the lipid bilayer, but weakly associated with proteins already attached, and neglect it in our analysis. The temperature of the measuring chamber was 25.2 ± 0.2 ° C.

The protein adlayer is formally characterized by its geometrical thickness $d_{\mathcal{A}}$ and isotropic refractive index $n_{\mathcal{A}}$ [10,11], which can be obtained from the measured N_{TE} and N_{TM} by simultaneously solving the corresponding mode equations [20,10,11]. $d_{\mathcal{A}}$ and $n_{\mathcal{A}}$ can be combined to yield the number ν of adsorbed molecules per unit area [10,11]:

$$\nu = \frac{d_{\mathcal{A}}(n_{\mathcal{A}} - n_C)}{m(dn/dc)} \,, \tag{2}$$

where n_C (= 1.332 742) is the refractive index of the aqueous cover (i.e., the buffer in which the proteins are dissolved), and m the mass of a single protein molecule, equal to 9.38×10^{-20} and 9.78×10^{-20} g for 1A2 and 2B4, respectively [21]. The value of the coefficient dn/dc was determined for the related protein cytochrome b5 (which was available in larger quantities than 1A2 and 2B4) with an LI3 Rayleigh interferometer (Zeiss, Jena, Germany) as 0.163 cm^3/g. The uncertainty in ν was ±10 molecules μm^{-2}.

Proteins. Cytochrome P450 1A2 and 2B4 were purified to electrophoretic homogeneity from the liver microsomes of New Zealand rabbits treated with 3-methylcholanthrene (for 1A2) or phenobarbital (for 2B4) by the methods of Imai *et al.* [22] and Karuzina *et al.* [23], respectively.

Lipids and other reagents. Synthetic DOPC was purchased from Avanti Polar Lipids, Alabaster, AL. The buffer (*p*H 7.2) was 0.01 M N-2-hydroxyethylpiperazine-N'-2-ethanesulfonic acid (Sigma Chemical Co.)–NaOH

(analytical grade) plus 0.1 M NaCl in "Nanopure" (Barnstead, Dubuque, IO) water.

III. RESULTS AND DISCUSSION

The flux F to an empty surface is given by [24,10]

$$F = c_b(2D_3/3)^{2/3}[\mathcal{F}/(xRA)]^{1/3} , \quad (3)$$

where D_3 is the translational diffusion coefficient in solution and c_b the bulk protein concentration, which was accurately determined from the absorption spectrum of protein solution reduced with sodium dithionite in the presence of carbon monoxide using an extinction coefficient of 91 mM^{-1} cm^{-1} for the difference between the maximum absorption in the 450 nm region and at 490 nm [25]. x, R, and A are the dimensions of the flow-through cuvette: distance x from the inlet pipe to the measuring spot = 3.5 mm; radius R = 1 mm; and cross-sectional area $A = 1.7$ mm^2.

If the proteins were to attach themselves to the membrane and immobilize themselves, then the simple RSA model would apply, according to which the rate of deposition is

$$d\nu/dt = Jc_b\phi , \quad (4)$$

where $J = F/c_b$ is the specific flux per unit bulk concentration and ϕ the available area function which takes into account the areas excluded from further absorption by proteins already adsorbed. Up to a surface coverage $\theta \approx 0.3$, ϕ is well approximated by the following polynomial [5,6]:

$$\phi = 1 - 4\theta + \frac{6\sqrt{3}}{\pi}\theta^2 + b\theta^3 , \quad (5)$$

where $b = 1.406\ 88$ and θ and ν are related by

$$\theta = \nu a , \quad (6)$$

a being the area per adsorbed molecule. Globular proteins adsorbing irreversibly and immoveably onto smooth mineral surfaces show excellent agreement with RSA kinetics [26]. If the surface configuration of particles is in equilibrium, maintained through the particles being mobile at the surface [6] or being able to desorb [9], the coefficient b in Eq. (5) equals 2.4243 [6].

Plotting the experimental data as $d\nu/dt$ vs ν (Fig. 3), we observed that *at the same molar concentrations* 2B4 (×) shows the characteristic curvature of RSA [Eqs. (4) and (5)], whereas 1A2 (□) yields a straight line given by (4) and the Langmuir expression

$$\phi = 1 - \theta , \quad (7)$$

that is, the entire unoccupied area of the surface is available for the adsorption of fresh particles. Since the lipid bilayer presents a continuum to protein adsorption, this behavior can only arise if the adsorbed molecules are grouped together in large, compact clusters such that the excluded area is a negligible fraction of θ. By increasing the bulk solution concentration of 1A2, we found the behavior switched from Langmuir to RSA. Conversely, by decreasing the concentration of 2B4, we observed a switch from RSA to Langmuir kinetics. Were the clustering to arise by molecules attaching with high probability whenever they landed on the surface contiguous to (touching) an already adsorbed molecule, and with low probability elsewhere, we would expect the shape of the kinetic curve to be independent of bulk concentration. Hence, the pathway to clustering appears to be via diffusion on the surface. Surface rearrangement leading to clustering cannot take place faster than surface diffusion, and will take longer if not every collision between adsorbed molecules leads to a cluster.

The characteristic time for rearranging the surface by lateral diffusion is $\tau_d = 1/(D_2\nu)$, where D_2 is the lateral diffusion coefficient. The equivalent time for adsorption from the bulk is $\tau_a = 1/(Jc_b\phi a)$. Present measurements for D_2 of proteins adsorbed to a lipid bilayer in the liquid-crystalline phase, are $\sim 10^{-9}$ cm^2/s [27], i.e., somewhat lower than values reported for the lipid molecules themselves ($\sim 10^{-8}$ cm^2/s) [28]. Furthermore, the coefficient D_2 will depend on θ according to [29]

$$D_2 \approx D_2^{(0)} \exp[-\chi(4+\chi)\xi - \chi(2+\chi)\xi^2] , \quad (8)$$

where $D_2^{(0)}$ is the coefficient for an infinitely dilute system, χ is a constant for a given type of particle and estimated at 0.3 for the P450 proteins, and $\xi = \theta/(1+\theta)$ (this equation assumes that the particles are randomly distributed rather than clustered). These times τ_a and τ_d may be compared using a parameter ζ introduced by Tarjus *et al.* [9] and defined as

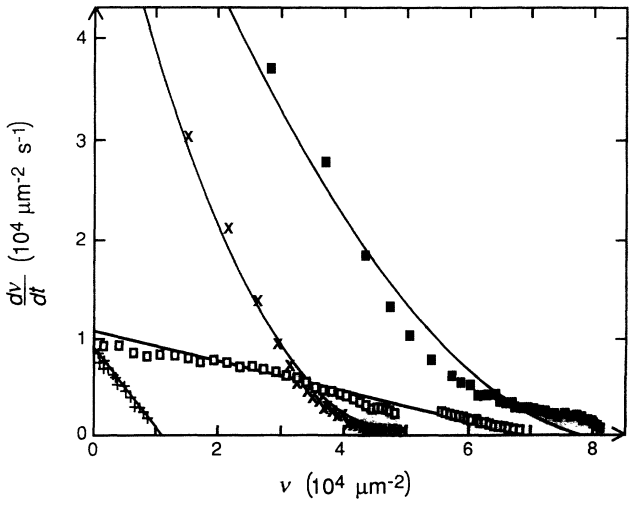

FIG. 3. Plots of $d\nu/dt$ vs ν. ■, 1A2, 3 μM; □, 1A2, 0.3 μM; ×, 2B4, 0.3 μM; +, 2B4, 0.0045 μM (ordinate values multiplied by 20 to make them visible on the given scale). Solid lines: fitted data (see Table I for parameter values).

TABLE I. Parameters derived from fitting experimental data to RSA or Langmuir kinetics.

Protein	c_b (nmol cm^{-3})	$\mathcal{F}$ (mm^3 s^{-1})	D_3(cm^2 s^{-1})	a(nm^2)	model	ζ
1A2	0.3	2.0	4.0×10^{-7}	14.2	Langmuir	0.7
1A2	3.0	1.6	2.6×10^{-7}	5.6	RSA	0.2
2B4	0.0045	1.8	2×10^{-6}	24	Langmuir	0.9
2B4	0.3	2.1	5.5×10^{-6}	9.2	RSA	0.2

$$\zeta = \frac{\tau_a}{\tau_a + \tau_d} = 1/\left(1 + \frac{Jc_b\phi a}{D_2\nu}\right) . \quad (9)$$

For a pure RSA process with no surface diffusion, $\zeta = 0$; as surface diffusion becomes more important, ζ approaches unity. The inverse dependence of ζ on c_b provides the easiest way to vary ζ. Hence, we increased the concentration of 1A2 tenfold. The result, also shown in Fig. 3 (■) *is an RSA curve*. Decreasing the concentration of 2B4 tenfold still resulted in RSA behavior; decreasing it sixtyfold (Fig. 3, +) resulted in Langmuir behavior.

Data were fitted to either (4), (5), and (6) using J and a as fitting parameters, or to (4), (6), and (7), where J and a are given by the intercepts. Parameter values are given in Table I. Since, according to (3), all the parameters determining J except D_3 are known, D_3 was calculated using (3) from the fitted values of J.

To estimate ζ from (9) and (3) we first have to determine J. For this we used the following parameters: $\langle\mathcal{F}\rangle = 1.9$ mm^3/s and x, R, and A as given above. D_3 does not appear to have been experimentally determined before; we estimate it from the Stokes-Einstein relation,

$$D_3 = \frac{k_BT}{3\eta}\left(\frac{\rho}{6\pi^2 m}\right)^{1/3} , \quad (10)$$

where η is the viscosity of the solution (8.9×10^{-4} N s/m^2) and ρ the protein density, for which we take a value of 1.35 g/cm^3 [30]. This calculation yields $D_3 \approx 10^{-6}$ cm^2/s. Taking $\phi/\nu = 10^3$ cm^2/nmol and $\langle a\rangle = 13$ nm^2, we find that with $c_b = 0.3$ nmol/cm^3 and $D_2 = 10^{-10}$ cm^2/s, $\zeta \approx 0.7$. This corresponds to the Langmuir kinetics observed with 1A2 ($\zeta \to 1$). Increasing c_b tenfold while leaving the remaining parameters unchanged gives $\zeta \approx 0.2$, corresponding to the observed RSA kinetics ($\zeta \to 0$). To obtain the same value of ζ at $c_b = 0.3$, corresponding to the RSA kinetics observed with 2B4 at this concentration, we need to put $D_2 = 10^{-11}$ cm^2/s. Decreasing c_b to 0.0045 nmol/cm^3 then results in $\zeta \approx 0.9$. These values are summarized in Table I.

Therefore, it appears that a roughly tenfold difference, in either the coefficients of lateral diffusion of 1A2 and 2B4 or the probabilities that a collision between two adsorbed molecules diffusing laterally leads to attachment, is sufficient to account for the observed kinetics. The difference must have its origin in the differing amino acid sequences of the two proteins, which might have been thought to be trivial. We are presently rather far from being able to predict the consequences of such small differences.

It should be noted that the Langmuir kinetics consistently yield bigger values of a compared with the RSA kinetics, implying some area-increasing conformational changes upon clustering. Some conformational change has previously been observed upon incorporation of the protein into the lipid bilayer [31]. Also, the behavior of 1A2 deposited from high bulk concentration at the highest coverages measured does not follow RSA kinetics very well; the observed deviation may indicate that an ordered configuration has formed [9].

ACKNOWLEDGMENT

This work was supported by the Human Frontier Science Program Organization and the International Science Foundation.

[1] M.C. Bartelt and V. Privman, Int. J. Mod. Phys. **5**, 2883 (1991).
[2] J.W. Evans, Rev. Mod. Phys. **65**, 1281 (1983).
[3] A. Rényi, Magy. Tud. Akad. Mat. Kut. Int. Közl. **3**, 109 (1958).
[4] J. Bafaluy, B. Senger, J.-C. Voegel, and P. Schaaf, Phys. Rev. Lett. **70**, 623 (1993).
[5] P. Schaaf and J. Talbot, Phys. Rev. Lett. **62**, 175 (1989).
[6] P. Schaaf and J. Talbot, J. Chem. Phys. **91**, 4401 (1989).
[7] Y. Pomeau, J. Phys. A **13**, L193 (1980).
[8] R. Swendsen, Phys. Rev. A **24**, 504 (1981).
[9] G. Tarjus, P. Schaaf, and J. Talbot, J. Chem. Phys. **93**, 8352 (1990).
[10] J.J. Ramsden, J. Stat. Phys. **73**, 853 (1993).
[11] J.J. Ramsden, Q. Rev. Biophys. **27**, 41 (1994).
[12] D.R. Nelson, T. Kamataki, D.J. Waxman, F.P. Guengerich, R.W. Estabrook, R. Feyereisen, F.J. Gonzalez, M.J. Coon, I.C. Gunsalus, O. Gotoh, K. Okuda, and D.W. Nebert, DNA Cell Biol. **12**, 1 (1993).
[13] V.Yu. Uvarov, V.E. Tretiakov, and A.I. Archakov, Phys. Chem. Biol. Med. **1**, 27 (1993).
[14] V.Yu. Uvarov, A.I. Sotnichenko, E.L. Vodovozova, J.G.

Molotkovsky, E.F. Kolesanova, Yu.A. Lyulkin, A. Stier, V. Krueger, and A.I. Archakov, Eur. J. Biochem. **222**, 483 (1994).

[15] A.I. Archakov, G.I. Bachmanova, M.K. Sandler, I.Yu. Tutochkin, and A.V. Lisitsa, in *Cytochrome P-450: Biochemistry and Biophysics,* edited by A.I. Archakov and G.I. Bachmanova (INCO-TNC, Moscow, 1992), pp. 673-679.

[16] J.J. Ramsden, J. Phys. Chem. **97**, 4479 (1993).

[17] A. Vašíček, *Optics of Thin Films* (North-Holland, Amsterdam, 1960).

[18] P.K. Tien, Rev. Mod. Phys. **49**, 361 (1977).

[19] A. Ghatak and K. Thyagarajan, *Optical Electronics* (Cambridge University Press, Cambridge, 1989).

[20] K. Tiefenthaler and W. Lukosz, J. Opt. Soc. Am. B **6**, 209 (1989).

[21] A.I. Archakov and G.I. Bachmanova, *Cytochrome P450 and Active Oxygen* (Taylor and Francis, London, 1991).

[22] T. Imai, C. Hashimoto-Yotsudo, H. Satake, A. Gerardin, and R. Sato, J. Biochem. **67**, 249 (1980).

[23] I.I. Karuzina, G.I. Bachmanova, D.E. Mengazetdinov, K.N. Myasoedova, G.P. Kuznetsova, and A.I. Archakov, Biokhimia **44**, 1049 (1979).

[24] V.G. Levich, *Physicochemical Hydrodynamics* (Prentice Hall, Englewood Cliffs, NJ, 1962).

[25] T. Omura and R. Sato, J. Biol. Chem. **239**, 2370 (1964).

[26] J.J. Ramsden, Phys. Rev. Lett. **71**, 295 (1993).

[27] N.L. Thompson, K.H. Pearce, and H.V. Hsieh, Eur. Biophys. J. **22**, 367 (1993).

[28] L.K. Tamm and H.M. McConnell, Biophys. J. **47**, 105 (1985).

[29] A.P. Minton, Biophys. J. **55**, 805 (1989).

[30] P.A. Charlwood, J. Am. Chem. Soc. **79**, 776 (1957).

[31] A.I. Archakov, V.Yu. Uvarov, G.I. Bachmanova, A.G. Sukhomudrenko, and K.N. Myasoedova, Arch. Biochem. Biophys. **212**, 378 (1981).